



Searches for Charginos and Neutralinos in e^+e^- Collisions at $\sqrt{s} = 161$ and 172 GeV

The ALEPH Collaboration

Abstract

The data recorded by the ALEPH detector at centre-of-mass energies of 161, 170, and 172 GeV have been analysed for signals of chargino and neutralino production. Events consistent with the expectation from Standard Model processes were observed in the data. No evidence for a signal was found. Limits are derived on the production cross sections and extended to interpretation in the Minimal Supersymmetric Standard Model. The limit on the mass of the lightest chargino is $85.5 \text{ GeV}/c^2$ for gaugino-like charginos ($\mu = -500 \text{ GeV}/c^2$), and $85.0 \text{ GeV}/c^2$ for Higgsino-like charginos ($M_2 = 500 \text{ GeV}/c^2$), for heavy sneutrinos ($m_0 \geq 200 \text{ GeV}/c^2$) and $\tan \beta = \sqrt{2}$. The effect of light sleptons is investigated, and limits are derived for both the chargino and neutralino analyses under that scenario. Assumptions of universal scalar or gaugino masses have been relaxed, allowing less model-dependent limits to be obtained.

Submitted to the 1997 EPS-HEP conference, Jerusalem

1 Introduction

In 1996, LEP opened a new energy regime in e^+e^- collisions at and above the W pair production threshold. This increased centre-of-mass energy allows for the direct search of new physics phenomena, in particular for supersymmetric particles.

Supersymmetry (SUSY) [1] associates to every ordinary particle a partner differing by half a unit of spin. Gauginos are associated to the ordinary gauge bosons, Higgsinos to the Higgs bosons, sleptons, sneutrinos and squarks to the ordinary matter fermions. Neutral Higgsinos and gauginos mix to form mass eigenstates called neutralinos, $\chi, \chi', \chi'', \chi'''$, in order of increasing mass. Similarly, charged gauginos and Higgsinos form charginos, χ^\pm and χ_2^\pm . The relevant MSSM parameters are M_1 and M_2 (the gaugino masses associated to the $U(1)$ and $SU(2)$ gauge groups), μ (the supersymmetric Higgs mass term), and $\tan\beta$ (the ratio of the two Higgs v.e.v.). R-parity, a multiplicative quantum number distinguishing between ordinary and supersymmetric particles, is assumed to be conserved. As a consequence, supersymmetric particles are produced in pairs and decay to the Lightest Supersymmetric Particle (LSP), assumed here to be the lightest neutralino, which is weakly interacting and does not decay, escaping detection.

In this paper, the Minimal Supersymmetric Standard Model (MSSM) is used as a reference model, but the results generally apply in a broader framework. Unless otherwise specified, unification of the gaugino masses at the GUT scale is assumed, leading to the relation $M_1 = 5/3 \tan^2 \theta_W M_2$. Similarly, a universal scalar mass m_0 is assumed for all sfermions, as well as a universal trilinear coupling at GUT scale. A special effort has been undertaken to interpret the results in a larger framework, relaxing the gaugino mass and/or the scalar mass unification assumptions.

With unification of gaugino mass terms, in the region where $M_2 \gg |\mu|$ the lightest chargino and neutralino have large Higgsino components; this is referred to as the Higgsino region. Similarly, the region where $|\mu| \gg M_2$ is referred to as the gaugino region. The region of small negative μ and low M_2 is referred to as the mixed region.

In this paper, searches for charginos and neutralinos are reported, based on data collected by ALEPH from July to November 1996: 10.8 pb^{-1} at $\sqrt{s} = 161.3 \text{ GeV}$, 1.1 pb^{-1} at 170.3 GeV and 9.6 pb^{-1} at 172.3 GeV .

2 Searches for Charginos and Neutralinos

At LEP, charginos are pair produced by virtual photon or Z exchange in the s -channel, and sneutrino exchange in the t -channel. The s - and t -channels interfere destructively, such that low sneutrino masses lead to smaller cross sections. Neutralinos are produced by s -channel Z exchange and t -channel selectron exchange. Here, s - and t -channels interfere constructively, for most of the parameter space. As a consequence, cross sections are higher if selectrons are light.

Charginos decay to a neutralino and a lepton-neutrino or quark-antiquark pair. If all sfermions are heavy (large m_0), the decay proceeds mainly through the exchange of a virtual W. The dominant final state topologies for chargino pair production are then: hadronic events with missing energy carried away by the two neutralino LSP's, called here the four jet topology (4J); a hadronic system accompanied by a lepton (2JL topology). Acoplanar lepton pairs (AL topology) are also produced,

but at a much lower rate. The second lightest neutralino χ' decays to a neutralino and a fermion-antifermion pair. If all sfermions are heavy, the decay proceeds mainly through the exchange of a virtual Z. The main final state resulting from $\chi\chi'$ production therefore consists mainly of acoplanar jets (AJ), due to the small Z leptonic branching ratio.

Selections for the 4J, 2JL and AJ topologies have been designed for chargino and neutralino masses close to the kinematic limit for $\chi^+\chi^-$ or $\chi\chi'$ production, and optimised for such W^* (Z^*) exchange dominated decays and for various ΔM ranges. Here ΔM is the mass difference between the chargino or the second lightest neutralino and the lightest neutralino. The signal properties (and the background composition) change dramatically with the mass difference: for low ΔM , the phase space for decay is small and the signal topology resembles $\gamma\gamma$ production, while, for very large ΔM , as is the case for massless neutralinos, the signal for chargino production is more WW-like. Small mass differences are typical of the Higgsino region while large mass differences tend to correspond to the gaugino region.

The chargino analyses in the 4J and 2JL topologies have been designed for four ΔM regions: very low (VL) for $\Delta M \simeq 5 \text{ GeV}/c^2$, low (L) for $\Delta M \simeq 10 \text{ GeV}/c^2$, high (H) ($\Delta M \simeq M_{\chi^+}/2$) and very high (VH) ($\Delta M \simeq 80 \text{ GeV}/c^2$). The efficiencies as a function of ΔM for the chargino analysis are shown in Fig. 1, separately for the ‘‘H’’ (both charginos decay to $q\bar{q}\chi$) and ‘‘M’’ (one chargino decays to $\ell\nu\chi$ ($\ell = e, \mu, \tau$) and the other to $q\bar{q}\chi$) signal topologies. The efficiencies for the different topologies are combined according to the appropriate branching ratios to give an overall efficiency; here, W branching ratios are applied.

In the case of neutralino production, $\chi\chi'$ production is the only relevant process in the Higgsino region. Two neutralino analyses in the AJ topology (AJ-L and AJ-H) have been designed for ΔM smaller than or greater than $30 \text{ GeV}/c^2$. For other sets of MSSM parameters, in particular in the mixed region, the heavier neutralinos χ'' , χ''' can also be produced. Complex topologies arising from cascade decays and from $\chi' \rightarrow \chi\gamma$ are addressed by a number of dedicated selections: 4 Jets with Photons (4J-H and 4J- γ), Acoplanar Leptons (AL), and Multileptons (ML).

For low values of m_0 , leptonic chargino and neutralino decays are enhanced, due to the increased influence of slepton exchange diagrams. (No signal for squarks has been found at the Tevatron so it is expected that squarks are heavy, and they should not influence chargino and neutralino decays. Theoretically, they are expected to be heavier than sleptons because of the larger radiative corrections to their masses.) The dominant topologies are then acoplanar lepton pairs (and multi-leptonic events), and the selections are inspired from those designed for the slepton searches[2]. If m_0 is low enough, two-body decays such as $\chi^+ \rightarrow l\tilde{\nu}$ or $\chi' \rightarrow \nu\tilde{\nu}$ open up (the latter leading to an invisible final state).

In the various selections, the cuts are adjusted according to the ‘‘ \bar{N}_{95} prescription’’, as explained in Ref.[3]. The optimal compromise between signal efficiency and background level is obtained when the expected 95% C.L. excluded signal production cross section is minimal, based on Monte Carlo simulations; this optimum changes, *i.e.* the cuts become tighter, as the integrated luminosity increases. For any given chargino and neutralino mass combination (or any choice of M_2 , μ and $\tan\beta$), and for any given leptonic branching ratio (or any choice of m_0), an optimal combination of the various selections is then chosen, again according to the \bar{N}_{95} prescription.

3 Results

3.1 Events selected in the data

In the 21 pb⁻¹ data taken at $\sqrt{s} = 161\text{-}172$ GeV, 7.3 events are expected from background in the chargino selections, and 3.8 in the neutralino selections. There is some overlap in the background expectations for the chargino and neutralino analyses. A total of fifteen events are observed in the data, with some events selected by both the chargino and neutralino analyses, and several events selected in other ALEPH searches for Supersymmetry [2, 4].

The number of events selected in the data, their distribution among the selections and their properties do not suggest a signal for Supersymmetry. Therefore, limits are set on the production of charginos and neutralinos, and constraints placed on the parameters of the MSSM. The candidate events are taken into account in deriving the limits in the regions of (M_{χ^\pm}, M_χ) and $(M_{\chi'}, M_\chi)$ in which the analyses that select each candidate are applied. No background subtraction is performed, except in the AL selection for two-body chargino decay, where the WW background is subtracted [5].

3.2 Limits on the production cross section

Upper limits on sparticle production cross sections can be derived from the results of these searches. Unless sleptons are light, W* exchange dominates the decay of charginos, so the process $e^+e^- \rightarrow \chi^+\chi^- \rightarrow W^*\chi W^*\chi$ defines the signal topology used to set upper limits on the cross section in the plane of M_{χ^\pm} and M_χ , shown in Fig. 2. The efficiencies used in the derivation of this limit were estimated for $\mu = -500$ GeV/c², $\tan\beta = \sqrt{2}$. The features of the contours of constant cross section reflect discontinuities in the number of candidates at points where the combinations of selections change and where the additional luminosity from data taken at lower energies applies. The integrated luminosities taken at centre-of-mass energies of 130, 136 [6], 161, and 170 GeV are scaled by the ratio of cross sections in the gaugino region to those at 172 GeV, and included with the data taken at 172 GeV to derive this limit. Due to radiative corrections to the chargino cross section, scaling by the ratio of cross sections in the gaugino region rather than the Higgsino region leads to a more conservative result.

3.3 Interpretation in the MSSM

3.3.1 Standard scenario: heavy sleptons

Chargino and neutralino masses and cross sections are determined by the parameters μ and M_2 , for a given value of $\tan\beta$ and m_0 (assuming the gaugino mass unification relation between M_1 and M_2). Limits on the production of charginos and neutralinos constrain these parameters, as depicted in Fig. 3 for two values of $\tan\beta$ and for $m_0 = 200$ GeV/c². This choice of m_0 gives $M_{\tilde{\nu}} \gtrsim 190$ GeV/c², which is conservative in the heavy slepton scenario as the chargino cross section is reduced significantly compared to higher values of m_0 . In the gaugino region, the chargino production cross section is high, and selection efficiency is high since $\Delta M \simeq M_{\chi^\pm}/2$. Charginos are excluded nearly to the kinematic limit, as seen in Fig. 5a. The limit on the chargino mass is 85.5 GeV/c² for $\mu = -500$ GeV/c² and $\tan\beta = \sqrt{2}$. In the Higgsino region, the cross section is lower and ΔM is small, leading to a lower selection efficiency due to the difficulties of minimising $\gamma\gamma$

background, and slightly weaker limit ($M_{\chi_{\pm}} > 85 \text{ GeV}/c^2$ for $\Delta M > 10 \text{ GeV}/c^2$). The additional gain from the search for $\chi\chi'$ production, which is most powerful in the Higgsino region for low $\tan\beta$, is also shown. In the mixed region, for chargino production, ΔM increases, and the selection efficiency is lower due to the difficulty of eliminating the WW background. For high $\tan\beta$, the exclusion from the chargino search reaches the kinematic limit, and no additional exclusion is gained from the neutralino search. In the following, the discussion will be concentrated on the low $\tan\beta$ case.

The impact of the neutralino search is seen more clearly in Fig. 4. The limit on the chargino mass as a function of M_2 is derived using the chargino and neutralino analyses separately. For lower M_2 , charginos are excluded nearly to the kinematic limit by the chargino search alone. The neutralino analysis allows exclusion beyond the kinematic limit for chargino production. Charginos and neutralinos constitute independent signals in this region, and the expected signals and numbers of candidates are summed to obtain a combined limit, extending the exclusion in the Higgsino region, as shown in Fig. 4. This is most evident in the deep Higgsino region, where the combination of chargino and neutralino analyses sets a limit on the chargino mass above $79 \text{ GeV}/c^2$, for $M_2 \leq 1200 \text{ GeV}/c^2$ (corresponding to $\Delta M \geq 5 \text{ GeV}/c^2$). This improves the limit of $72 \text{ GeV}/c^2$ set by the chargino search alone.

3.3.2 Effects of light sleptons

The effect of low slepton masses is significant in both the production and decay of chargino and neutralinos, as explained in Section 2. Here limits are derived from the chargino and neutralino searches when sleptons are light and the particular role played by staus is clarified.

Light sleptons, nominal stau mixing

The limit on the chargino mass throughout the gaugino region has been evaluated as a function of μ for several values of m_0 and for $\tan\beta = \sqrt{2}$, as shown in Fig. 5a. This limit is derived from the chargino analysis assuming a universal scalar mass, m_0 , for the sleptons. The overall reduction in the limit for decreasing m_0 is due to the diminished cross section. Stau mixing, as will be discussed later, has been calculated with $A_\tau = 0 \text{ GeV}/c^2$.

The evaluation of low m_0 effects is extended to the (μ, M_2) plane, as shown in Fig. 5b. The effect in the gaugino region, as seen in the previous plot, is also evident in the mixed region, where a “valley” for $-\mu \approx M_2$ opens up in the region excluded by chargino searches. There is a modest improvement in the excluded region from charginos as m_0 increases from $200 \text{ GeV}/c^2$ to $1000 \text{ GeV}/c^2$. In the Higgsino region, light scalars have little effect on the exclusion obtained with the chargino and neutralino searches, and all limits are similar to high m_0 results. In contrast to chargino production, the neutralino cross section increases dramatically as m_0 is reduced below $100 \text{ GeV}/c^2$. The results cover the chargino valley and slightly improve the LEP 1 limit. The limits from neutralino searches for $m_0 = 75 \text{ GeV}/c^2$ are expressed as a limit on the chargino mass in Fig. 5a.

In chargino production and decay for low m_0 , the relevant physical quantity is the mass of the sneutrino, as this determines the reduction in cross section and enhancement of the leptonic branching ratio. Therefore, the limit on the chargino mass can be meaningfully expressed as a

function of the sneutrino mass. As seen in Fig. 6 for two points in the gaugino region, when $M_{\tilde{\nu}} \geq 150 \text{ GeV}/c^2$, there is little effect due to the sneutrino mass or stau mixing; this is similar to the case under which the limits in Figs. 3 and 4 were derived. In the near gaugino region ($\mu = -80 \text{ GeV}/c^2$), light sleptons have less of an effect on the leptonic branching ratio; the limit in this case is lower than for $\mu = -500 \text{ GeV}/c^2$ due to the lower cross section. (See also Fig. 5.)

When $M_{\tilde{\nu}} \leq M_{\chi^\pm}$, two-body decays, $\chi^\pm \rightarrow \ell\tilde{\nu}$, tend to dominate. When $M_{\chi^\pm} - M_{\tilde{\nu}} \leq 3 \text{ GeV}/c^2$, the leptons do not have enough energy to pass the selection, and no exclusion is obtained. This is the ‘‘corridor’’ visible at low $M_{\tilde{\nu}}$ in Fig. 6. The differences in the corridor for these two points are due to the effects of stau mixing, as will be discussed in the following sub-section. Also shown is the limit from the slepton search [2], which excludes the corridor where no limit can be obtained from the chargino search. The slepton limit is derived for $\tan\beta = \sqrt{2}$ and $\mu = -100 \text{ GeV}/c^2$, and is much weaker for high $\tan\beta$; thus, a general exclusion of this region is difficult.

Effects of stau mixing

Due to the relatively high mass of the tau lepton, mixing between the left- and right-handed staus can occur, modulated by the off-diagonal term in the stau mass matrix, $m_\tau(A_\tau - \mu \tan\beta)$. The lightest stau, $\tilde{\tau}_1$, can be significantly lighter than the other sleptons and sneutrinos, causing an increase in the branching ratios of charginos and neutralinos to final states with taus. The decay amplitude also depends on the field content of the chargino or neutralino, and is most enhanced in the gaugino region. Thus, the most evident effects of stau mixing are observed for gaugino-like charginos and neutralinos.

The impact of stau mixing is shown in Fig. 7, where the limit on the chargino mass as a function of sneutrino mass has been derived assuming a universal slepton mass, for three values of the tri-linear coupling term, A_τ . A point in the deep gaugino region is chosen, specifically $\mu = -500 \text{ GeV}/c^2$, for $\tan\beta = \sqrt{2}$. For high $M_{\tilde{\nu}}$, there is little effect from stau mixing, and the results are as discussed previously. As $M_{\tilde{\nu}}$ decreases, $M_{\tilde{\tau}_1}$ decreases, with a relative mass splitting which depends on A_τ .

For $A_\tau = 0$, $\tilde{\tau}_1$ is slightly lighter than the $\tilde{\nu}$, so two-body decays, $\chi^\pm \rightarrow \tilde{\tau}_1\nu$, occur when $\chi^\pm \rightarrow \ell\tilde{\nu}$ is kinematically forbidden. When the $\tilde{\nu}$ becomes light enough, $\chi^\pm \rightarrow \ell\tilde{\nu}$ decays are allowed, although some fraction of the decays will remain $\chi^\pm \rightarrow \tilde{\tau}_1\nu$. This causes the partial recovery of the corridor. When $M_{\tilde{\nu}}$ is lower, $\chi^\pm \rightarrow \ell\tilde{\nu}$ decays dominate.

Two extreme cases for the impact of stau mixing were considered, setting A_τ to $+1 \text{ TeV}/c^2$ and $-1 \text{ TeV}/c^2$. For a given $(M_{\chi^\pm}, M_{\tilde{\nu}})$ point, $\tilde{\tau}_1$ is heavier for $A_\tau = +1 \text{ TeV}/c^2$ than for $A_\tau = 0$. As a consequence, the branching ratio to taus is reduced and limits are stronger for $M_{\tilde{\nu}} > M_{\chi^\pm}$; on the other hand, there are no $\chi^\pm \rightarrow \tilde{\tau}_1\nu$ decays to fill in the corridor. The situation is reversed for $A_\tau = -1 \text{ TeV}/c^2$, where limits are lower for $M_{\tilde{\nu}} > M_{\chi^\pm}$ but where $\chi^\pm \rightarrow \tilde{\tau}_1\nu$ decays exclude the region of sneutrino masses just below the chargino mass.

The limits from the chargino analysis are derived for low $\tan\beta$. For high $\tan\beta$, in the gaugino region, staus become tachyonic for low $M_{\tilde{\nu}}$, so this case is not considered.

3.3.3 Non-universal scalar masses

The results shown in Fig. 7 rely on the assumption that the slepton masses unify at the GUT scale, as expected in many SUSY GUT models. In chargino decays, the sneutrino and left sleptons are most relevant; the pure right slepton plays no role. Therefore, theoretical constraints relating the masses of the left and right sleptons and sneutrinos can be dropped, retaining simply $M_{\tilde{\ell}L}^2 = M_{\tilde{\nu}}^2 - M_{\tilde{W}}^2 \cos 2\beta$, which is guaranteed by gauge invariance. In this framework, the results previously derived from the chargino search are still valid aside from the stau mixing effects.

When the chargino decays to three bodies, the most conservative limit is obtained when the highest possible branching ratio to final states with taus occurs (leading to the lowest efficiency) thereby maximising the impact of stau mixing. This is achieved by varying the $\tilde{\tau}_1$ mass and mixing angle to obtain the highest branching ratio for three body decays to $\tau\nu\chi$ (without relying on a universal scalar mass, m_0 , for mass relations among the sleptons, or constraints on A_τ) and the result is shown in Fig. 7. This limit is derived for $\mu = -500 \text{ GeV}/c^2$, as gaugino-like charginos are more sensitive than Higgsino-like charginos to the effects of stau mixing. This can be compared to the cases discussed previously for several values of A_τ . Since the chargino selections have good sensitivity for final states with taus, the limit in this worst case is not very different from the other examples.

3.3.4 Non-universal gaugino masses

If the unification relation between M_1 and M_2 is assumed, the mass difference between the chargino and lightest neutralino depends on the parameters of the MSSM: in the gaugino region, ΔM is $\simeq 40 - 50 \text{ GeV}/c^2$; for low negative μ and M_2 , ΔM can be higher; in the Higgsino region ΔM becomes very small. Fig. 8a shows the limit on chargino mass throughout the range of ΔM which can be attained in the gaugino and Higgsino region.

If the gauge unification condition is relaxed, the tight correspondence between the χ^\pm and χ masses in the gaugino region can be broken. Varying M_1 and M_2 independently, the limit on the chargino mass is displayed as a function of ΔM in Fig. 8a, for $\tan\beta = \sqrt{2}$. The two hatched bands show the spread in the limit as μ is varied between -500 and $-80 \text{ GeV}/c^2$, for heavy sleptons, and maximising the impact of stau mixing as described in Section 3.3.3. Defining $\alpha = M_1/\frac{5}{3} \tan^2\theta_W M_2$, the plot shows the range $0.01 < \alpha < 10$. The reach of the search into the region of very high ΔM is shown; for a nearly massless neutralino, the limit on the chargino mass is $82 \text{ GeV}/c^2$. These limits change little with $\tan\beta$, and are valid for high m_0 ($\geq 200 \text{ GeV}/c^2$).

The limits for several values of sneutrino mass have been evaluated, and the exclusion in the (M_{χ^\pm}, M_χ) plane is shown in Fig. 8b. In addition to relaxing gaugino mass unification, scalar mass unification has been relaxed, and the maximum impact of stau mixing has been taken into account. These limits are independent of assumptions on a universal slepton or gaugino mass at the GUT scale, requiring only that charginos decay to three bodies.

4 Conclusion

The data recorded with the ALEPH detector at centre-of-mass energies of 161, 170, and 172 GeV have been examined for signals of chargino and neutralino production. Selections sensitive to

topologies arising from chargino production were developed for a wide range of mass difference between the chargino and lightest neutralino, and especially, for very high and very low ΔM . Additional selections were developed for topologies arising from chargino and heavier neutralino decays when sleptons are light. In all of the chargino analyses, 7.3 events were expected, and in the neutralino analyses, 3.8 events were expected, with some overlap between the background expectations. A total of 15 candidate events was observed in the data; more events than expected were selected by analyses with background from WW and two-photon processes. These events are consistent with Standard Model processes, and no evidence of a signal is claimed.

Limits on the production of charginos and neutralinos have been derived, and interpreted in the context of the MSSM. The diversity of topological selections and breadth of sensitivity allow interpretation under a variety of model assumptions. Limits have been derived assuming unification of gaugino masses and heavy sleptons, giving exclusion of charginos essentially to the kinematic limit. The light slepton scenario has been explored, and limits on chargino and neutralino production derived. The effects of stau mixing have been taken into account, including relaxing the requirement of a universal scalar mass to obtain a limit independent of SUSY GUT models. In addition, the gaugino mass unification condition has been relaxed, allowing limits to be derived on the chargino mass which are independent of assumptions on the mass relations among sleptons and gauginos at the GUT scale, requiring only that no sleptons are lighter than the chargino.

References

- [1] for an introduction to Supersymmetry, see for example H.E. Haber and G.L. Kane, Phys. Rep. **117** (1985) 76.
- [2] ALEPH Coll., *Search for sleptons in e^+e^- collisions at centre-of-mass energies of 161 GeV and 172 GeV*, CERN **PPE/97-056**.
- [3] ALEPH Coll., *Phys. Lett.* **B384** (1996) 427.
- [4] ALEPH Coll., *Searches for Scalar Top and Scalar Bottom Quarks at LEP2*, submitted to the 1997 EPS-HEP conference, Reference number 622.
- [5] Particle Data Group, Phys. Rev. **D 54**,(1996).
- [6] ALEPH Collaboration, *Phys. Lett.* **B373** (1996) 246.

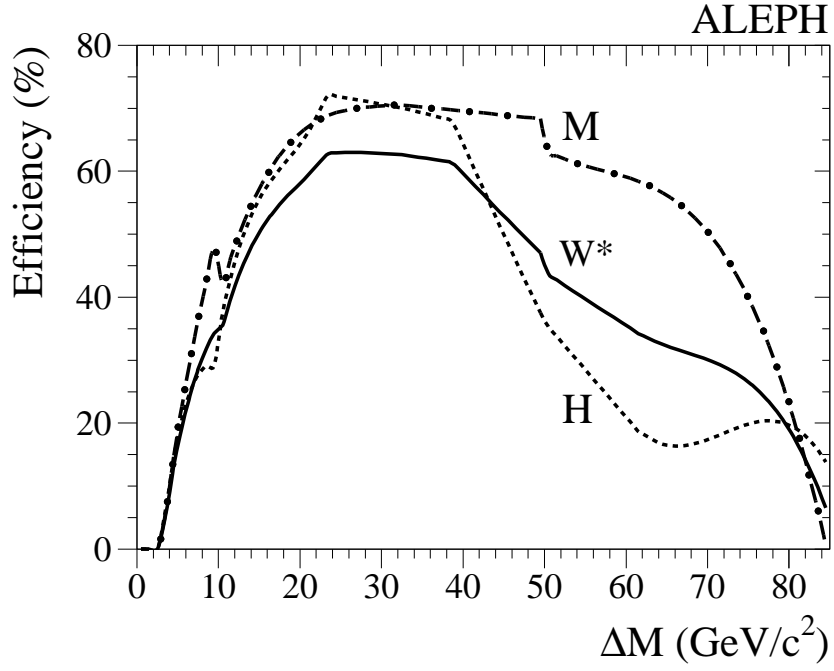


Figure 1: *Parametrised selection efficiency for the chargino selections. The efficiency is plotted as a function of ΔM , for $M_{\chi^\pm} = 85 \text{ GeV}/c^2$ at $\sqrt{s} = 172 \text{ GeV}$, measured for $\mu = -500 \text{ GeV}/c^2$ and $\tan \beta = \sqrt{2}$. Efficiencies are plotted for mixed ('M') and hadronic ('H') topologies, and combined assuming W branching ratios, $Br(\chi^\pm \rightarrow \ell \nu \chi) = 0.33$ ('W*').*

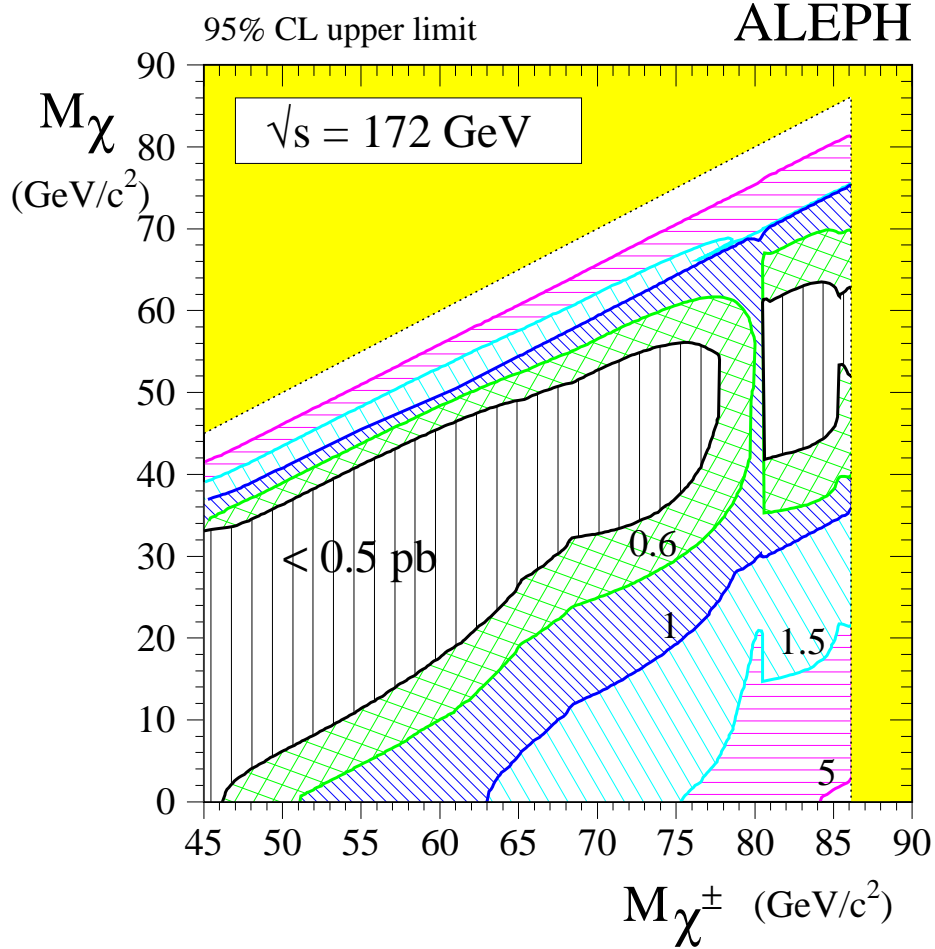


Figure 2: The 95% C.L. upper limit on the cross section for chargino pair production, in the (M_{χ^\pm}, M_χ) plane. Data taken at lower centre-of-mass energies (130, 136, 161, and 170 GeV) are included by scaling the luminosity by the ratio of the cross section at that energy to the cross section at $\sqrt{s}=172$ GeV, for $\mu = -500$ GeV/c² and $\tan\beta = \sqrt{2}$. W branching ratios are assumed in the chargino decay.

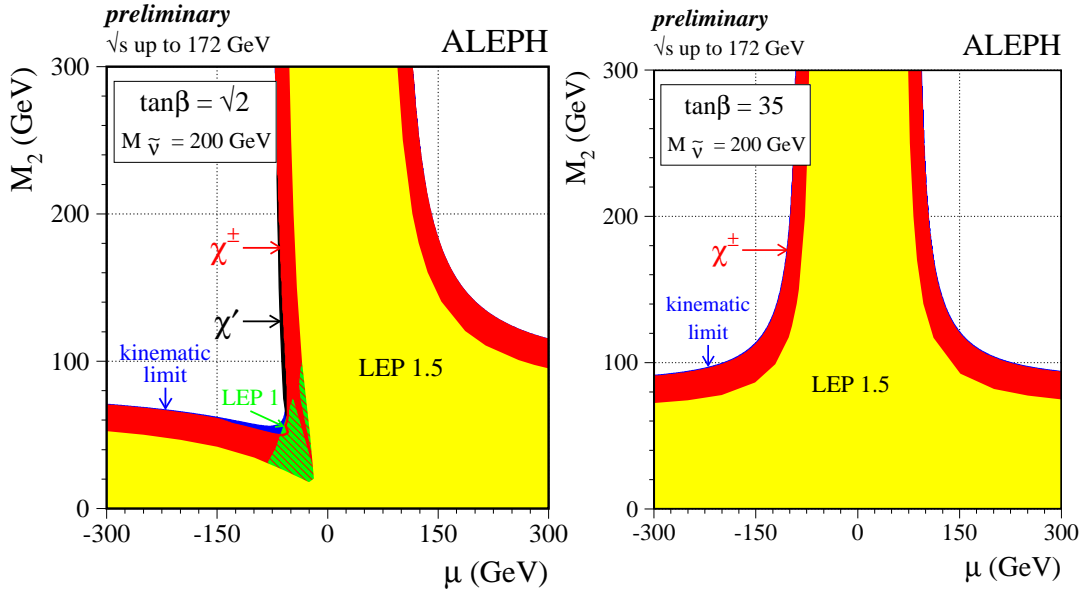


Figure 3: *Exclusion in the (μ, M_2) plane, for $\tan\beta = \sqrt{2}$ and 35, and $M_{\tilde{\nu}} = 200 \text{ GeV}/c^2$.*

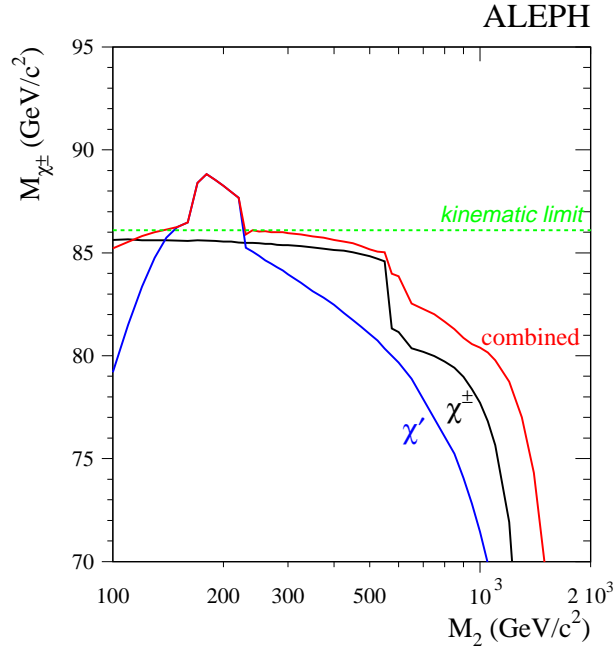


Figure 4: *The limit on the chargino mass as a function of M_2 , from the chargino search (labelled χ^\pm), from the neutralino search (labelled χ'), and from the combination of chargino and neutralino searches. This limit is derived for $\tan\beta = \sqrt{2}$.*

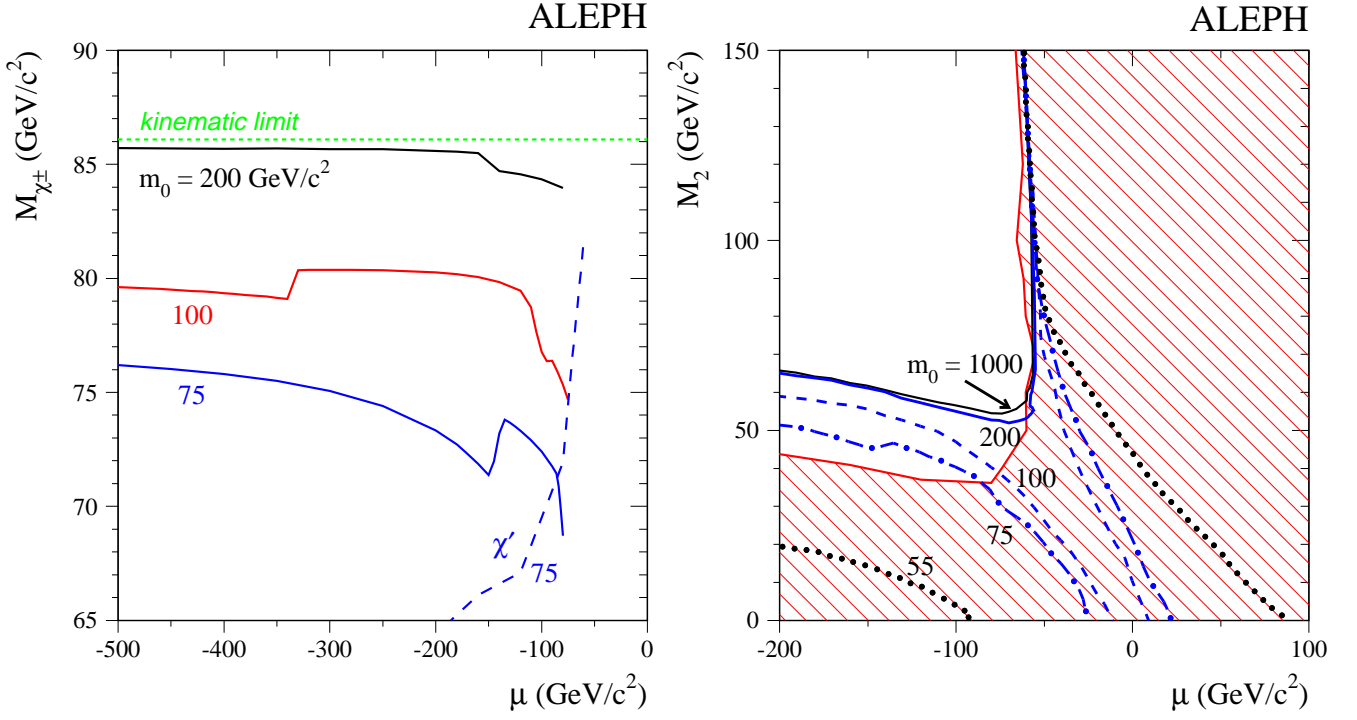


Figure 5: On the left is the limit on the chargino mass as a function of μ , for several values of m_0 . The excluded chargino mass from the neutralino search for $m_0 = 75 \text{ GeV}/c^2$ is shown as a dashed line. On the right, the exclusion in the (μ, M_2) plane for several values of m_0 is shown. The dark lines indicate limits from the chargino searches, and the hatched area is the exclusion from the neutralino analysis, for $m_0 = 75 \text{ GeV}/c^2$. These limits are derived for $\tan\beta = \sqrt{2}$.

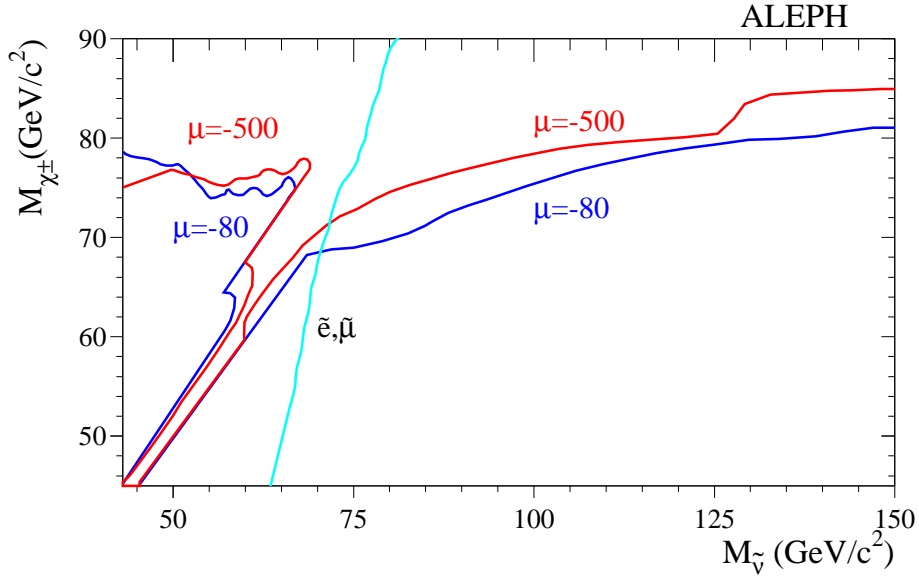


Figure 6: The limit on the chargino mass as a function of sneutrino mass in the gaugino region, evaluated for $m_{\chi^\pm} < m_{\tilde{\nu}}$, for $\tan\beta = \sqrt{2}$ and $A_\tau = 0$. The limit from selectron and smuon searches for $\tan\beta = \sqrt{2}$ and $\mu = -100 \text{ GeV}/c^2$ is also indicated.

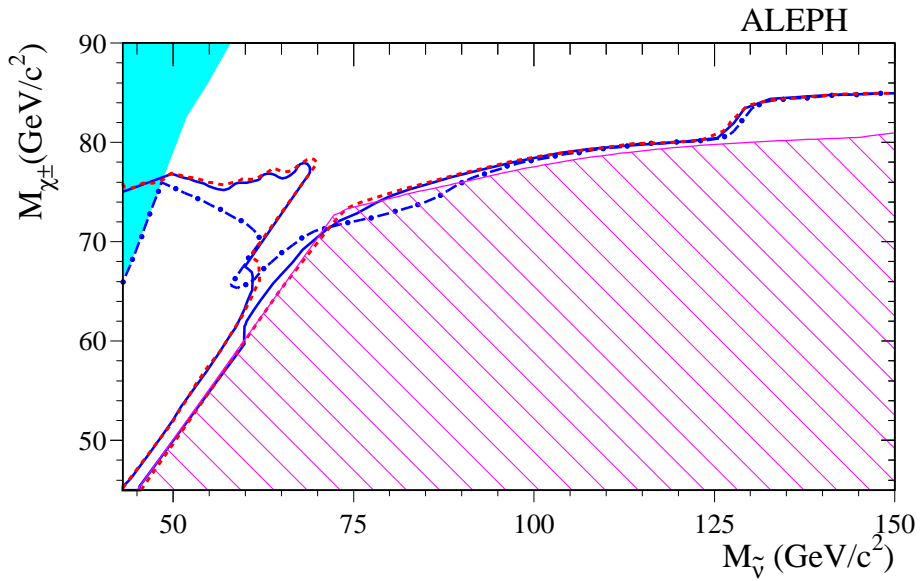


Figure 7: *The limit on the chargino mass as a function of sneutrino mass, for $\mu = -500 \text{ GeV}/c^2$ and $\tan \beta = \sqrt{2}$. First, a universal scalar mass is assumed, and the limit is derived for $A_\tau = 0$ (solid line), $A_\tau = +1 \text{ TeV}/c^2$ (dashed line) and $A_\tau = -1 \text{ TeV}/c^2$ (dot-dash line). Second, the assumption of a universal m_0 is dropped, and the impact of stau mixing is maximised (for three-body chargino decays), shown as the slanted hatched region. The shaded region at low $M_{\tilde{\nu}}$ is theoretically forbidden for $A_\tau = -1 \text{ TeV}/c^2$.*

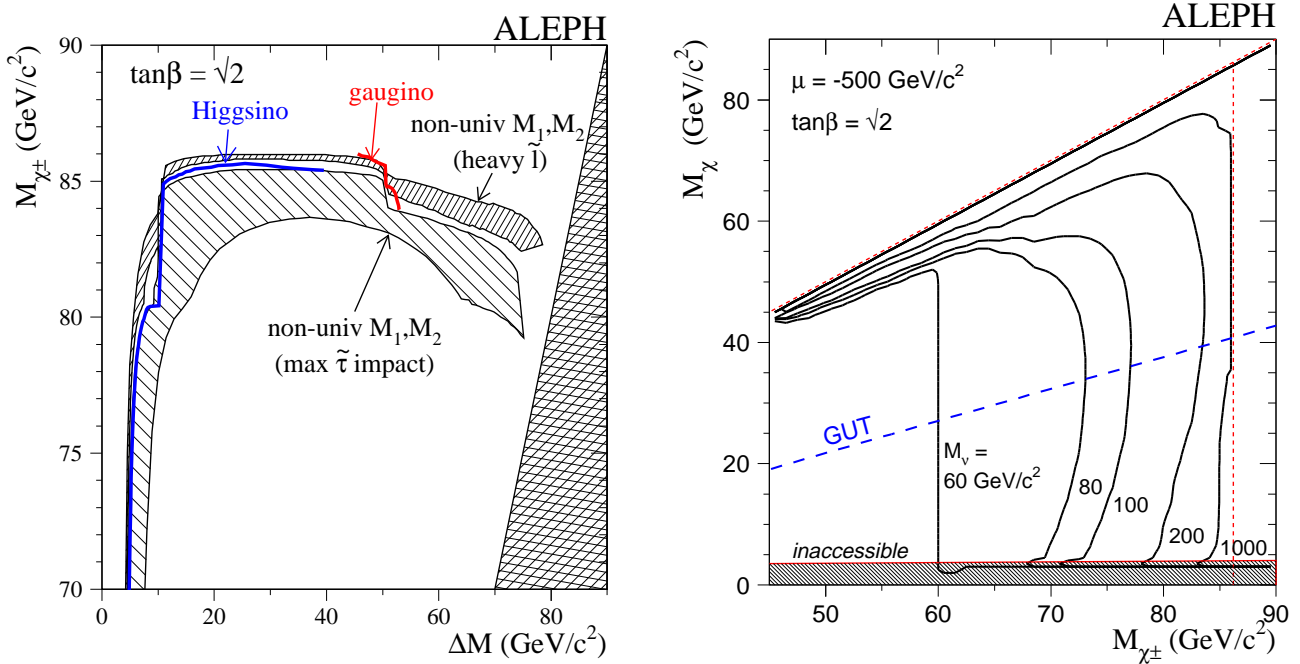


Figure 8: On the left, the limit on the chargino mass as a function of ΔM , for $M_{\tilde{\nu}} \geq 200 \text{ GeV}/c^2$. The solid lines indicate the limit in the higgsino and gaugino regions, assuming gaugino mass unification. The shaded regions reflect the spread in the limits if gaugino mass unification is relaxed, as μ is varied from -80 to $-500 \text{ GeV}/c^2$, for heavy sleptons, and maximising the impact of stau mixing. On the right, the limit is shown in the (M_{χ^\pm}, M_χ) plane, relaxing gauge unification relations for the gaugino and slepton masses, for several values of $M_{\tilde{\nu}}$. The inaccessible region for very low M_χ can not be attained by relaxing the gauge unification relation.